JOURNAL OF OPTOELECTRONICS AND ADVANCED MATERIALS Vol. 8, No. 3, June 2006, p. 1012 - 1015

# Microstructure and humidity sensitive properties of $MgFe_2O_4$ ferrite with Sn and Mo substitutions prepared by selfcombustion method

C. DOROFTEI[a,b*], E. REZLESCU[b], N. REZLESCU[b], P. D. POPA[b]
[a]*Faculty of Physics, Al. I. Cuza University , Carol I Boulevard RO-700506,IasI,Romania*
[b]*Institute of Technical Physics, Bd. D. Mangeron 47, 700050 Iasi, Romania*

The study was focused on $MgFe_2O_4$ ceramic compound and it was investigated the influence of Sn and Mo ions which partly replaced Fe and Mg on the microstructure and humidity sensitivity of the electrical resistivity. We preferred the Mg based ferrite because: i) it is a slightly porous ceramic and ii) its high resistivity can support large humidity variations (over three orders of magnitude). In addition, the stability of $Mg^{2+}$ ions avoids the appearance of $Fe^{2+}$ ions which participate to the conduction process in the ferrite.

(Received March 15, 2006; accepted May 18, 2006)

*Keywords:* Humidity sensor, Ferrite, $MgFe_2O_4$, Sn, Mo substitution, Self-combustion method

## 1. Introduction

Humidity sensors based on semiconducting oxides have certain advantages compared to other types of humidity sensors, such as low cost, simple construction, small size and ease of locating the sensor in the operating environment. Basically, a ceramic sensor can detect humidity on the principle of measuring a change in the resistance by water vapor adsorption. The change in the resistance of the sensor can be explained by the fact that water molecules act as an electron-donating gas [1]. When water molecules are adsorbed on semiconductive oxide, the conductivity increases or decreases according to wheather the oxides are of n-type or p-type. This means that electrons are apparently transfered from water molecules to oxides. The ability of a metal oxide to sense the presence of water molecules depends on the interaction between water molecules and the surface of the metal oxides, i.e. the reactivity of its surface. The reactivity depends on composition and electronic and morphologic structure [2]. These surface characteristics are heavily affected by the preparation procedure and composition. Much interest was focused on Mg ferrite owing to its high electrical resistivity and high porosity [2,3].

In our previous papers [4-7] we have shown that various ferriets including Mg-based ferrites with different doping elements are sensitive to gases and humidity.

In this work we study the influence of the compositional change by substitutions on the morphology and electrical properties of Mg ferrite. This allowed us to correlate the results with sensitivity towards water vapors. As substituents we selected two ions, $Sn^{4+}$ and $Mo^{6+}$, with different sizes and valencies, which partially substituted Mg and/or Fe in $MgFe_2O_4$.

## 2. Experimental

The chemical formula for the ferrite compositions is: $Mg_{1-x}Sn_xFe_{2-y}Mo_yO_4$, where x and y have the values:

x = 0 and y = 0 (sample 1); x = 0.1 and y = 0 (sample 2); x = 0 and y = 0.02 (sample 3).

The samples were obtained by selfcombustion method using metal nitrate and ammonium hydroxide as raw materials. The coprecipitation of the metal hydroxides takes place into a colloidal medium. By a quick combustion takes place the calcinations of metal hydroxides and the reaction between metal oxides [8]. This procedure offers the advantage to produce ultra-fine, homogeneous and reproducible ferrite powders by using aqueous solutions of constituent ions (metal nitrates) salts, in comparison with conventional ceramic technology.

The as-prepared powder was compacted in a disk shape, by uniaxial pressing The compacts were sintered at 1100 $^oC$ for 4 h, in air. After sintering, the weight and dimensions of the shrinked pellets were measured, at room temperature, to determine sintered density, porosity and volume shrinkage.

The phase composition of the sintered pellets was identified by the standard X-ray diffraction (XRD), using CuKα radiation. The microstructure was examined by the scanning electron microscopy (SEM). The average grain size was determined by the linear-intercept technique from micrographs on the fracture surface of the samples. The specific surface area was calculated using the following equation

$$A = \frac{s}{v.d} = \frac{6}{Dm \cdot d}, \qquad (1)$$

where s and v are the particle surface and volume, respectively and d is the experimental density and Dm is the average grain size.

To measure the electrical properties of the samples, silver electrodes were applied to opposite faces of the disks. The alternating current electrical resistance was measured by a two-point method, with a LCR meter, at 100 Hz.

For the humidity sensing measurements the sensor element (silvered ferrite disc) was placed in a termostated enclosure and exposed to different relative humidities. Relative humidities ranging 11% to 98% were obtained using saturated salt solutions as the humidity generation source. A list of saturated salts and their constant humidity values is given in Table 1.

*Table 1. Relative humidity RH above saturated salt solutions at 20 °C.*

| Salt | LiCl | $K(C_2H_3O_2)$ | $MgCl_2$ | $K_2CO_3$ | $Mg(NO_3)_2$ | $CoCl_2$ | NaCl | KCl | $K_2SO_4$ |
|---|---|---|---|---|---|---|---|---|---|
| Relative Humidity ( % ) | 11.3 | 22.7 | 33.1 | 43.2 | 53.0 | 64.0 | 75.7 | 85.1 | 97.6 |

The resistance of the sensors was measured in dry air (about 0% RH) as well as in different humidities. During the measurements, the temperature was kept at 20 °C. After each change of the humidity, the sensor element was exposed to the new humidity for 2 minutes, before to measure the new resistance.

The humidity response times were obtained by monitoring the resistance changes when the relative humidity was varied from 53% to 98% and from 98% to 53%. To examine stability of the sensors, the humidity-resistivity characteristics at 20 °C, between 11% and 98% RH were measured after 10, 20 and 30 days and no important changes were observed. In fact, the sensor resistance slightly increased in room atmosphere after aging.

## 3. Results and discussion

Fig. 1 shows the X–ray diffractograms of samples. It is evident that only pure ferrite and Mo substituted ferrite are monophasic. The XRD lines belonging to the spinel structure are presented with Miller indices. In contrast to Mo ions, the Sn ion induces a foreign phase. This new phase has not yet been identified. Judging from the peak height, it seems that a large amount of foreign phase is present in the samples containing Sn (sample 2 compounds). The presence of the foreign phase can suggest a solubility limit of $Sn^{4+}$ ions in the spinel lattice due to its radius (0.083 nm [9]). It is known that the degree of replacement of the host cations by the other ions in the host lattice depends on the cationic radius of the substituents [10].

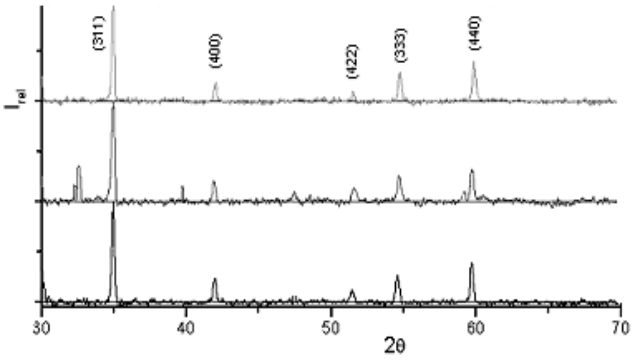


*Fig. 1. X-ray diffractograms for the studied: sample 1 ($MgFe_2O_4$), sample 2 ($Mg_{0.9}Sn_{0.1}Fe_2O_4$), sample 3 ($MgMo_{0.02}Fe_{1.98}O_4$).*

The values of lattice constant for cubic spinel structure of the investigated samples are listed in Table 2 (column 3). The slight changes in the lattice constants of the substitutional solid solutions should be attributed to the presence of $Sn^{4+}$ and $Mo^{6+}$ ions on the substitutional positions in the host ferrite lattice.

*Table 2. Structural data forthe investigated ferrites.*

| Sample | Cationic substituent | Lattice constant ( nm ) | Average grain size $D_m$ (nm) | Porosity ( % ) | Specific surface area A ($m^2/g$) |
|---|---|---|---|---|---|
| Sample 1 | No | 0.8354 | 500 | 45.8 | 5.0 |
| Sample 2 | Sn | 0.8352 | 100 | 51.6 | 23.8 |
| Sample 3 | Mo | 0.8334 | 310 | 46.3 | 8.9 |

When a cation whose radius and valence are different from those of the host cations is introduced into the spinel lattice, the ionic size mismatch between the host and dopant cations creates a strain in the lattice which can affect the unit cell size [10]. However, even for high doping level, such as sample 2, the lattice constant does not differ so much from that of the undoped ferrite. This fact reveals a good formed crystalline structure of spinel type.

Morpholgy of the sample can be vizualized from SEM micrographs on the fracture surfaces of the synthetized materials, as in Fig. 2. Each composition is characterized by a porous structure and submicronic rounded grains. It is evident that the structure of the Mg ferrite is affected by substitutions. The $SnO_2$ incorporation produced radical changes in microstructure (Fig. 2b). A substantial decrease in the grain size from 500 nm to about 100 nm and the formation of the grain bridges arround the interconected pores can be observed in Fig. 2b. Mo ions also affect the microstructure of the Mg ferrite (Fig. 2c) but in a smaller measure. It is possible that the presence of the foreign phase in the Sn-containing samples inhibits the grain growth.

The structural characteristic are summarized in Table 2. On can see that the Sn doped sample (sample 2) has the highest porosity, of 51%, and the largest specific area, of about 24 $m^2/g$. A larger specific area implies a much more active surface in front of water vapors and thus the sensitivity to humidity of the resistivity will be increased.

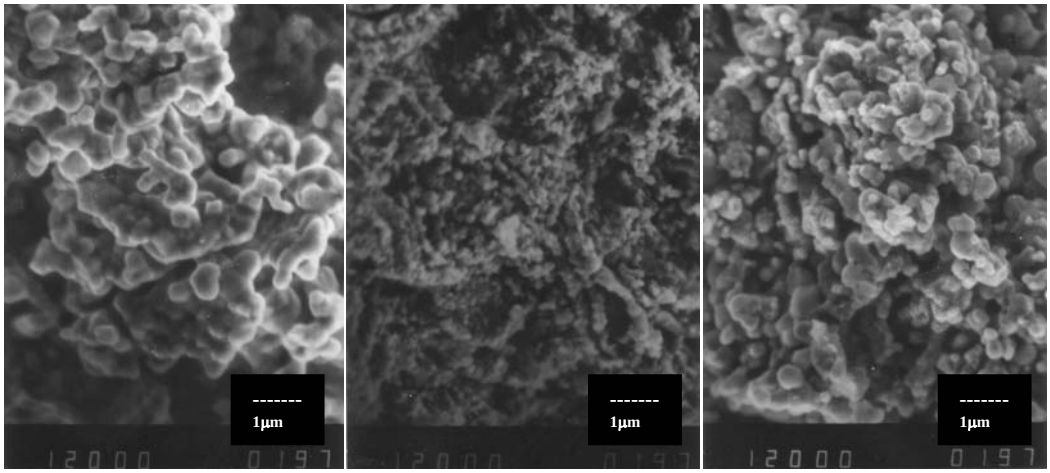


a b c

*Fig. 2. SEM micrographs the studied ferrites: a) Sample 1; b) Sample 2; c) Sample 3.*

The effects of the partial substitution of $Mg^{2+}$ and $Fe^{3+}$ of $MgFe_2O_4$ with $Sn^{4+}$ and $Mo^{6+}$ on the electrical resistivity humidity characteristics were also investigated as shown in Fig. 3. The following two observations can be made: i) The compositional changes of $MgFe_2O_4$ ferrite by Sn and Mo incorporation influence electrical resistivity of the material. Sn substituted ferrite (sample 2) exhibits the highest resistivity in dry air, of about $10^9$ Ω·cm, whereas Mo substituted ferrite (sample 3) has the smallest resistivity, of about $10^6$ Ω·cm. One can suppose that partial substitution of octahedral Mg ions by tetravalent Sn ions localizes the octahedral $Fe^{2+}$ ions and thus, the number of the electronic jumps between $Fe^{2+}$ and $Fe^{3+}$ (hopping conduction mechanism in ferrites) decreases [11].

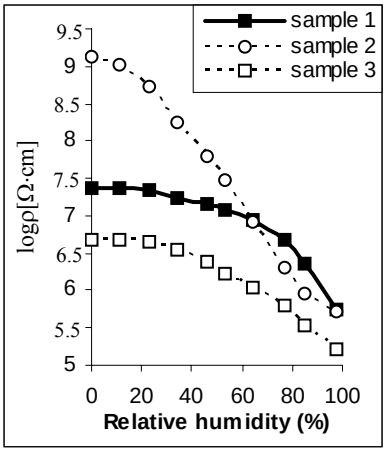


*Fig. 3. The resistivity –humidity characteristics for the investigated.*

Thus, the measurements show an increase in ρ with about two orders of magnitude as tin partially replaces magnesium in pure $MgFe_2O_4$ ferrite. Moreover, microstructure (porosity, grain size, structural defects) has a great role on the electrical resistivity. Smaller grains implie an increase of the grain boundary surface which normally account for high resistivity of a polycrystalline material. On doping with $Mo^{6+}$, the creation of the cation vacancies becomes predominant to maintain electroneutrality and in consequence, the electrical resistivity will decrease as a result of dissociation of oxygen in the vecinity of cation vacancies .

ii) The humidity sensitivity depends upon the microstructure. The larger the specific surface area and porosity of the specimens the more water vapors can be physically adsorbed, resulting in a larger decrease of the resistivity. One can see from Fig. 3 that the Sn-substituted ferrite (Sample 2) is the most sensitive material to humidity change. The surface area of this element is the highest, of 23.8 $m^2/g$. Its electrical resistivity decreases by about three orders of magnitude, from $10^9$ Ω·cm to $10^6$ Ω·cm when the relative humidity increases from 11% to 85%. In addition, this result suggests that controlling the intrinsic resistance of the material is also an important factor in achieving excellent sensitivity to humidity.

In comparison with Sn substituted ferrite, the other ferrites exhibit a smaller decrease of the resistivity (Sample 1) and are sensitive to high relative humidities only, over 75%. It is thought that Sn ions become important with an increase in humidity. Their sensitivity at less than 43% RH is rather low. The unsubstituted ferrite improve the sensitivity to water vapors (humidity).

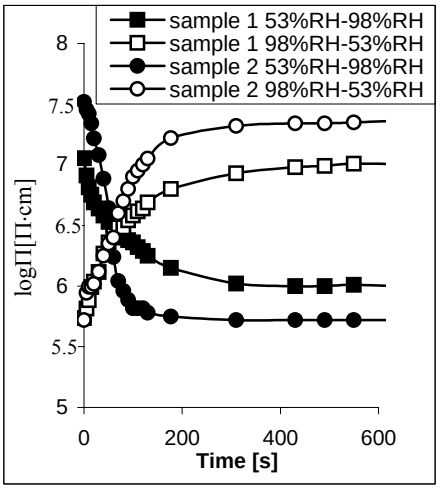


*Fig. 4. Humidity response characteristics for sample 1 and sample 2.*

The response rate of the electrical resistance due to humidity change was examined also. The humidity response characteristics to variation in RH from 53% to 98% and from 98% to 53% for $MgFe_2O_4$ (sample 1) and from 53% to 98% and from 98% to 53% for $Mg_{0.9}Sn_{0.1}Fe_2O_4$ (sample 2) are shown in Fig. 4. The response time of $MgFe_2O_4$ (sample 1) is of about 5 minutes to attain a steady state value of the resistivity, whereas the response time for $Mg_{0.9}Sn_{0.1}Fe_2O_4$ (sample2) is shorter, of about 3 minutes. These results may suggest that the adsorption or desorption rate of water vapors is controlled by the diffusion rate of these through the micropores which in its turn is dependent on the pore size distribution. Large micropores, above 0.5 μm, are necessary for rapid response to humidity changes. The $MgFe_2O_4$ element, which has a great number of micropores below 0.5 μm in diameter (Fig. 2a), showed a longer response time to humidity changes.

## 4. Conclusions

The influence of $Sn^{4+}$ and /or $Mo^{6+}$ ions on the microstructure and humidity sensitivity of the Mg ferrite prepared by selfcombustion method was studied.

The structure was investigated by XRD and SEM. The sintered compacts have a typical porous structure. The average grain size changes from 500 nm to 100 nm by partial substituting Mg with Sn ions in $MgFe_2O_4$.

The $Mg_{0.9}Sn_{0.1}Fe_2O_4$ porous ceramic exhibits the best humidity sensitivity among the specimen studied. Its electrical resistivity changed remarkably, by three orders of magnitude, when the relative humidity increased from 11% to 98%. Among the studied elements,this element exhibits a short response time. However, the response time is not yet satisfactory value.

These preliminary results show that the promoting effects of Sn ions on humidity sensitivity of Mg ferrite can be related with the changes in porosity and grain size (specific surface area).

Further investigations are necessary to shorten the response time, without any decrease in humidity sensitivity, and to explain the role of $Sn^{4+}$ substituent, which is responsible for the enhancement of the humidity sensitivity of Mg ferrite.

## References

[1] H. Arai, S. Ezaki, Y. Shimizu, O. Shippo, T. Seiyama, Semiconductive humidity sensor of perovskite-type oxides, Proc. Int. Meeting on Chemical Sensors, Fukuoka, Sept. 19-22, 393 (1983).
[2] Ding J. McAvoy Tj, Cavicchi RE, Semacik, Sensors and Actuators **B 77**, 597 (2001).
[3] T. Nitta, F. Fukushima, Y. Matuo, Proc. Int. Meeting on Chemical Sensors, Fukuoka, Sept. 19-22, 287 (1983).
[4] N. Rezlescu, E. Rezlescu, F. Tudorache, P. D. Popa, J. Optoelectron. Adv. Mater. **6**(2), 695 (2004).
[5] N. Iftimie, E. Rezlescu, P. D. Popa, N. Rezlescu, J. Optoelectron. Adv. Mater. **7**(2), 911 (2005).
[6] N. Rezlescu, E. Rezlescu, P. D. Popa, F. Tudorache, J. Optoelectron. Adv. Mater. **7**(2), 907 (2005).
[7] N. Iftimie, E. Rezlescu, P. D. Popa, N. Rezlescu, J. Optoelectron. Adv. Mater. **8**(3), 1016 (2006).
[8] P. D. Popa, N. Rezlescu, A new method for preparing $BaFe_{12}O_{19}$ ferrite powder, Romanian Reports in Physics **52**, 769 (2000).
[9] J. E. Huheey, E. A. Keiter, R. J. Keiter, Chemistry. Principles of structure and reactivity, Harper Collins, College Publishers, 1993.
[10] D. J. Kim, Lattice parameters, ionic conductivities, and solubility limits in fluorite-structure $MO_2$ oxide ($M = Hf^{4+}$, $Zr^{4+}$, $Ce^{4+}$, $Th^{4+}$, $U^{4+}$) solid solutions, J. Amer. Ceram. Soc. **72**, 1415 (1989).
[11] P. Kishan, N. Kumar, Magnetic behavior of LiMg ferrites with tetrava, Plent substituentsroc. Int. Symposium on Ferrites in Asia'97 (ISFA'97), J. Magn. Soc. Japan **22**, 21 (1998).

* Corresponding author: dcorneliu@yahoo.com